Applied Energy 204 (2017) 373–381

Contents lists available at ScienceDirect

Applied Energy

journal homepage: www.elsevier.com/locate/apenergy

The benefits and limitations of electrolyte mixing in vanadium flow batteries

Yunong Zhang [a], Le Liu [a,*], Jingyu Xi [a], Zenghua Wu [a], Xinping Qiu [a,b]

[a] Institute of Green Chemistry and Energy, Graduate School at Shenzhen, Tsinghua University, Shenzhen 518055, China
[b] Key Lab of Organic Optoelectronics and Molecular Engineering, Department of Chemistry, Tsinghua University, Beijing 100084, China

HIGHLIGHTS

- The benefits and limitations of electrolyte mixing method are studied in this work.
- Different current densities and mix times are studied.
- The VFB cycle number increases from 145 to 598 at 160 mA cm^{-2} by mixing the electrolytes.

GRAPHICAL ABSTRACT

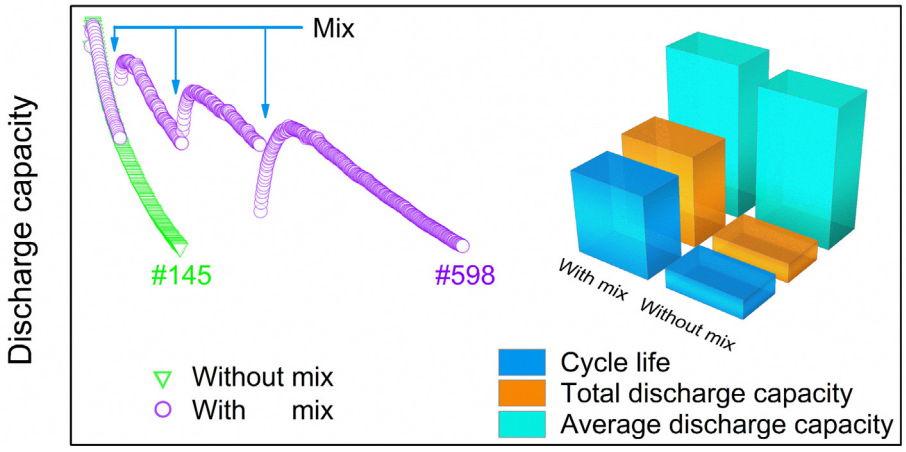

ARTICLE INFO

Article history:
Received 11 April 2017
Received in revised form 6 July 2017
Accepted 15 July 2017
Available online 25 July 2017

Keywords:
Vanadium flow battery
Electrolyte
Cycle life
Capacity regeneration
On-line monitoring

ABSTRACT

Cycle life prolongation and discharge capacity regeneration have drawn enormous attention in the field of vanadium flow batteries (VFBs). Among all the methods, mixing the positive and negative electrolytes is the most efficient, but the study about the proper time and the effect of the mix method is relatively deficient. In this study, different mix times and current densities are chosen to explore the benefits and limitations of the mix method, also the mechanism of discharge capacity behavior is discussed. Through the mix method, not only the cycle number has been extended significantly, but also the voltage and energy efficiencies are recovered. Although the contribution of the mix method is restrained by the average valence of the mixed electrolytes, it can be alleviated by electrolysis. The mix method is economic, uncomplicated and can be employed in industrial applications.

1. Introduction

Under the increasing pressure of population expansion and energy crisis, it is highly desirable to develop the utilization of renewable energy sources. As electrical energy storage (EES) plays a crucial role in the application of renewable energy sources and serves as a connection between the current electricity grid and fluctuating non-fossil energy sources, tremendous efforts have been made in the exploration of techniques for EES in recent years [1–6]. Proposed by NASA in 1970s, redox flow battery (RFB)

* Corresponding author.
E-mail address: liu.le@sz.tsinghua.edu.cn (L. Liu).

http://dx.doi.org/10.1016/j.apenergy.2017.07.049
0306-2619/

attracts considerable attention due to its good safety, fast response and separate design in power and energy [2,7–11].

To date, all-vanadium redox flow battery (VFB, VRB or VRFB), suggested by M. Skyllas-Kazacos and co-workers in 1980s [12], is regarded as one of the most promising large-scale energy storage systems for its long cycle life, flexible design, high efficiency and relatively low environmental impact [6,9,13–19]. Furthermore, the VFB system has been commercialized as a large-scale energy storage system [20,21]. Also, the technology, finance and policy aspects have been demonstrated [22]. In a VFB, the positive electrolyte (VO^{2+}/VO_2^+ in sulfuric acid solution) and the negative electrolyte (V^{2+}/V^{3+} in sulfuric acid solution) are reserved in the positive and negative reservoirs respectively, and are pumped into the cell stack to take part in electrochemical reactions [8,23]. Theoretically, VFB has a long cycle life, but it suffers severe capacity loss and performance degeneration, which is mainly resulted from electrolyte imbalance. The electrolyte imbalance is mainly caused by water and vanadium ions transfer through the separator as well as parasitic side reactions [24–26]. Owing to different permeability of vanadium ions with various oxidation states, non-equilibrium transfer of cations causes vanadium concentration imbalance in the positive and negative electrolytes. Meanwhile, difference between the chemical composition of the positive and negative electrolytes brings non-equilibrium transfer of water [27], leading to colossal volume change. Furthermore, V^{2+}, V^{3+}, VO^{2+} and VO_2^+ ions permeate through the separator with different number of bonded water molecules [15], aggravating the non-equilibrium transfer of water. In addition, side reactions including gas evolution, oxidation of V^{2+} ions by oxygen and precipitation formation of V_2O_5 endow the electrolyte imbalance by consuming electrons and available vanadium ions. Thus significant capacity loss and battery performance degeneration occur.

With such issues, there is emphasis on reducing the capacity decay rate of VFB. Thus pioneering studies about the mechanism of capacity decay and electrolyte composition change during the charge-discharge cycling process have been achieved, including water transfer and permeation of vanadium cations through membranes [27–30], thermal and dynamic modelling of battery configuration, self-discharge reactions, ion diffusion and side reactions [31,32], and the effects of electric field on ion crossover [33]. Together with working on the capacity decay mechanism, some advanced technologies have been employed to detect the component changes of electrolyte during the charge-discharge cycling process by monitoring state of charge (SOC) [34–36], transfer of active materials [37,38], oxygen evolution [39] and hydrogen evolution behaviors [40]. With the knowledge of theoretical modelling and virtual monitoring, it is easy to conclude that mitigating the ion transfer rate is one of the most efficient choices to reduce capacity decay rate. Hence, highly ion-selective separators have been suggested [41–47]. Although the rate of capacity decay can be alleviated significantly by the highly ion-selective separators, the non-equilibrium transfers of water and vanadium ions still exist, leading to electrolyte imbalance ultimately. To this end, burgeoning explorations have been made in operational conditions to regenerate capacity of VFB, such as tuning the sap pressure of the positive and negative electrolytes [48], employing asymmetric positive/negative electrolyte volumes [49], balancing the osmotic pressure of the electrolytes [50], altering the charging and discharge currents [51] and reflowing the electrolytes from the positive side to the negative side [52].

In the exploration process of regenerating discharge capacity, it is noteworthy that VFB system is free from cross-contamination as all the active materials are vanadium ions in the positive and negative electrolytes. This brings the possibility to regenerate VFB capacity by mixing the positive and negative electrolytes [8,53]. Although the mix method is uncomplicated and efficient, the study on the proper time of mix and the practical application value of mix method is relatively deficient. In this paper, the effect of mix method is studied, the benefits and limitations for prolonging battery cycle number are explored, and the mechanism of discharge capacity retention behavior is discussed. Comparing with other presented operational methods, the mix method studied in this paper is uncomplicated and economic.

2. Experimental section

2.1. Test system and parameter

The cycle number test system applied in this study was based on our previous works [54,55]. The digital photos and the schematic diagrams of a typical VFB system tested in this study are displayed in Fig. 1. Reservoirs, tubes, cells, flow controllers, peristaltic pumps and flow cuvettes were employed. The cell of the VFB contained two graphite polar plates (60 mm × 60 mm × 3 mm, Shanghai Hongfeng Industrial Co., Ltd), two pieces of graphite felts (50 mm × 50 mm × 5 mm, Gansu Haoshi Cabon Fiber Co., Ltd) and a Nafion 115 membrane (70 mm × 70 mm, Dupont). The graphite felts were washed in 50% ethanol solution, deionized water and then heated in the air at 420 °C for 10 h to improve hydrophilicity and electrochemical behavior. Nafion 115 membranes were treated in 3 wt% H_2O_2 solution, deionized water, 1 M H_2SO_4 solution and deionized water for 1 h in sequence. Flow cuvette was homemade with absorption depth of 1 mm. The positive and negative electrolytes containing 1.5 M vanadium ion (V^{3+}/VO^{2+} = 1:1) and 2.0 M free H_2SO_4 were 50 mL in all reservoirs initially. The peristaltic pump (BT 100 M, Baoding Chuangrui Precision Pump Co., Ltd) was used to control the flow rate of the positive and negative electrolytes at 60 mL min^{-1}. A battery test system (BTS CT-3008W, 5V6A, Neware Co., Ltd) performed the cycle number test in the voltage window of 1.65–0.80 V to avoid electrochemical corrosion on graphite polar plates and graphite felts. All the VFBs in this study were tested simultaneously under the same condition to exclude systematic error.

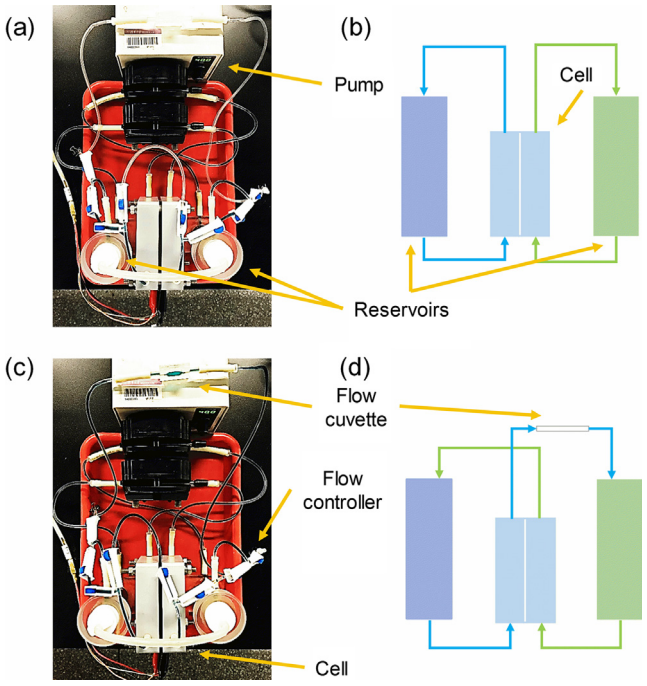

Fig. 1. (a, c) The photos of the normal work process and the mix process; (b, d) The schematic diagrams of the normal work process and the mix process.

2.2. Cycle number test process

As the current density may have influences on the side reactions, the behavior of vanadium permeation and the capacity decay rate, two different current densities (80 mA cm^{-2} and 160 mA cm^{-2}) were chosen in this experiment, in consideration of power and efficiency. In addition, considering of the maintenance frequency and the capacity requirement, mix process was conducted when discharge capacity retention went down to 75% or 50%. The mix process was performed after discharge to eliminate potential self-discharge.

Before the cycle number test, a pre-charge process was carried out to adjust the valence of vanadium ions into tetravalence at the positive side and trivalence at the negative side. When the discharge capacity retention of VFB-80/75 and VFB-160/75 decreased to 75%, or the discharge capacity retention of VFB-80/50 and VFB-160/50 decreased to 50%, the charge-discharge cycling process stopped and the running state of the batteries changed, so the electrolytes in the positive and negative reservoirs began to mix. During the mix process, the possibly formed precipitation of V_2O_5 can be depleted. After several minutes of mix, the average valence of the mixed electrolyte became stable, then the mixed electrolyte was divided equally into the positive and negative reservoirs. After that, the running state changed to normal work process, and a pre-charge process was applied. Then the charge-discharge cycling process restarted with mixed electrolytes. The mix process was performed each time the discharge capacity retention decreased to the selected level (75% or 50%) until the discharge capacity retention of the first cycle after the mix process was lower than that of the last cycle before the mix process. In comparison, VFB-80 and VFB-160 cycled without mix process and stopped when the discharge capacity retention decreased to 50%.

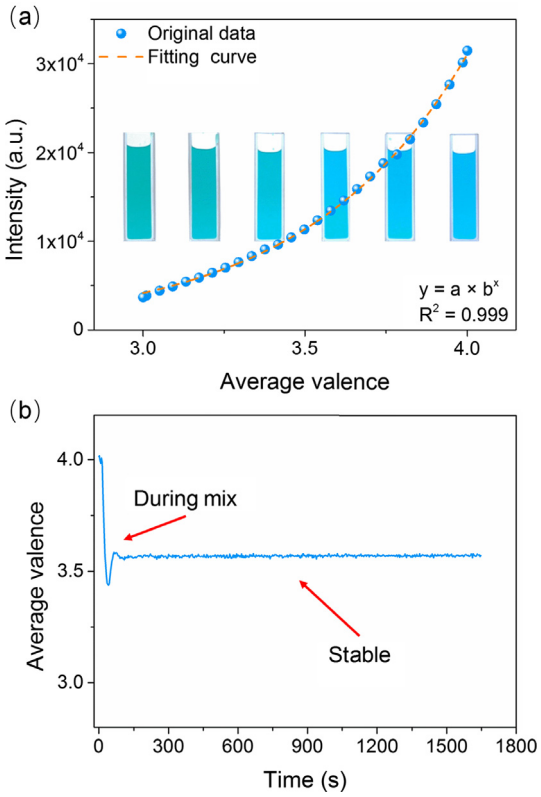

Fig. 2. (a) The relation between the transmitted light intensity at 445 nm and the average valence of the electrolyte. The curve fitting result is: a = 10.01, b = 7.465; (b) The average valence change of the mixing electrolytes during the first mix process of VFB-80/75.

2.3. Normal work process and mix process

Flow controllers used in medicine were employed to control the flow direction of the positive and negative electrolytes. As a result, the running state of VFBs can be divided into a normal work process and a mix process. Under the normal work process (Fig. 1(a, b)), the positive and negative electrolytes stored in the reservoirs are pumped into the cell separately, and the active materials take part in electrochemical reactions near the carbon electrodes. During the charge-discharge cycling process of VFBs with Nafion membranes, non-equilibrium transfer of water leads to imbalanced volume, which means the volume of positive electrolyte increases and the volume of negative electrolyte decreases. Meanwhile, different permeability of diverse vanadium ions leads to imbalanced vanadium concentration, causes net vanadium ions transfer from the negative to the positive electrolyte and brings self-discharge reactions. Moreover, the colossal changes of volume and vanadium ion concentration will not stop until almost all the negative electrolyte transfers to the positive side. After several cycles, the negative electrolyte with lower vanadium concentration and volume will limit the battery discharge capacity [49]. When the discharge capacity retention decreases to the selected level, the running state will be changed to mix process by switching the flow controllers. Under the mix process (Fig. 1(c, d)), the reservoir of the positive electrolyte is connected to the negative half-cell while the reservoir of the negative electrolyte is connected to the positive half-cell, which makes it possible to fully mix and equally divide the electrolytes.

The batteries tested in this study were denoted as VFB-80, VFB-80/75, VFB-80/50, VFB-160, VFB-160/75 and VFB-160/50. For example, VFB-80/75 meant cycling under the current density of 80 mA cm^{-2} and conducting the mix process when the discharge capacity retention decreased to 75%, while VFB-80 meant cycling under the current density of 80 mA cm^{-2} and without mix process.

2.4. Detection of the average valence of the mixed electrolyte

The on-line spectroscopic detection method introduced in our previous works [39,56] was employed to detect the optical absorption of the initial and the mixed electrolytes at the wavelength of 445 nm in the flow cuvette to obtain the average valence. With the self-developed spectroscopic detection system, a calibration experiment was performed to determine the relation between the transmitted light intensity (at 445 nm) and the valence of the electrolyte. Fig. 2(a) shows the experimental data and the fitting curve of this relation. With this curve, the average valence of the electrolyte can be calculated by detecting the transmitted light intensity.

During the mix process, electrolytes flowed into the flow cuvette and the transmitted light intensities were monitored to calculate the average valances. Fig. 2(b) shows the variation of the average valence of the electrolyte during the first mix process of VFB-80/75. From Fig. 2(b), it can be concluded that the average valence of the electrolyte changes dramatically at first and then become stable a few minutes later during the mix process.

3. Results and discussion

3.1. Discharge capacity, average valence and volume change

Discharge capacity retention is defined as the ratio of the discharge capacities of different cycles to the discharge capacity of the first cycle. The discharge capacity retentions of all six batteries are displayed in Fig. 3(a, e), the sudden changes of discharge capacity retentions are caused by mix processes. Take VFB-80/75 as an

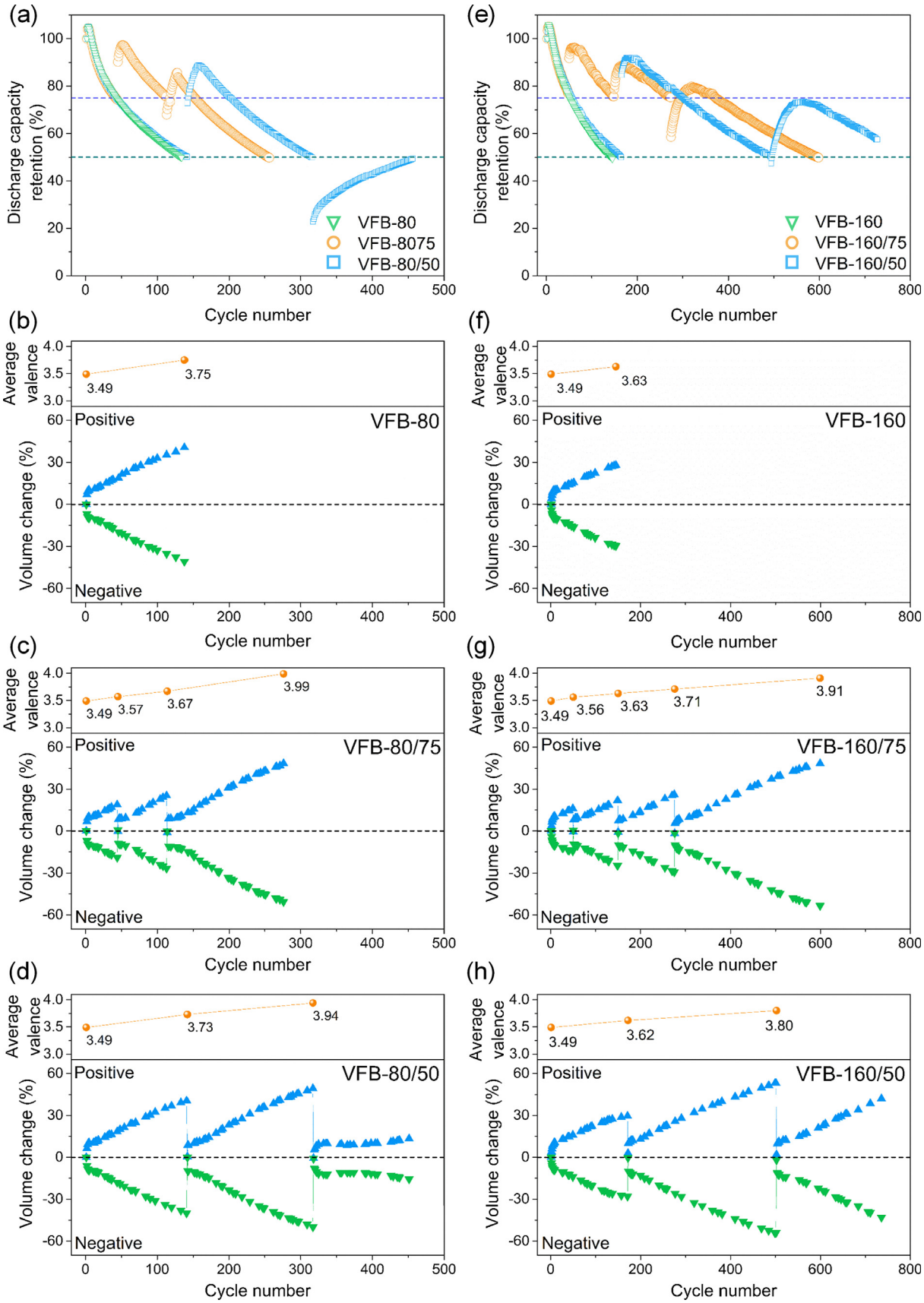

Fig. 3. (a, e) Discharge capacity retention of VFBs under current densities of 80 mA cm^{-2} and 160 mA cm^{-2}, respectively; (b–d) Average valences and volume changes of VFBs under current densities of 80 mA cm^{-2}; (f–h) Average valence and volume changes of VFBs under current densities of 160 mA cm^{-2}.

example (orange circles in Fig. 3(a)). At the beginning of the cycle number test, the discharge capacity decays with cycle number increase. Through the first mix process (at cycle 42), the discharge capacity recovers from 75% to near 90%, then increases for some cycles and decreases at last. When the discharge capacity retention decreases to 75% for the second time, mix process happens again (at cycle 113). Although the discharge capacity retention increases above 75% some cycles later after the second mix process, the discharge capacity retention of the first cycle after the second mix process is lower than that of the last cycle before the second mix process. In that case, no more mix process is conducted for VFB-80/75 and the battery stops running when the discharge capacity retention decreases to 50%. For other batteries, mix processes are conducted at cycle 142 and 317 for VFB-80/50; at cycle 50, 149 and 274 for VFB-160/75; at cycle 165 and 494 for VFB-160/50. Through this mix method, cycle number is increased from 134 (VFB-80) to 256 (VFB-80/75) and 316 (VFB-80/50) at the current density of 80 mA cm^{-2}, and is increased from 145 (VFB-160) to 598 (VFB-160/75) and 727 (VFB-160/50) at the current density of 160 mA cm^{-2}.

Fig. 3(b–d, f–h) shows the average valences and the volume changes during the cycle number test. The average valences of the mixed electrolytes are measured at the beginning of cycle number test, after each mix process and at the end of the cycle number test, and the volumes of the positive and negative electrolytes are recorded after charge-discharge cycles. The average valences of the mixed electrolytes increase with the cycle number. Since the transfer of active vanadium materials has no influence on the average valence of the mixed electrolyte, the increase may result from undesirable side reactions and possible leakage of air. Similarly, the volumes of the positive and negative electrolytes changes symmetrically with cycle number increase.

As showed in Fig. 3(b–d, f–h), the volumes of the positive electrolytes increase while the volumes of the negative electrolytes decrease, the volume changes tend to be sharp during original cycles and then more moderate during later cycles. Furthermore, the tendencies of the volume changes at different periods are broadly consistent, but a sudden change after the second mix process in VFB-80/50 is recorded. Connecting with the change of average valence, this behavior may result from the changed composition of mixed electrolytes. In addition, running batteries with electrolyte at high average valence can lead to accumulation of VO_2^+ ions at the positive side, causing severe precipitation of V_2O_5. The precipitation of V_2O_5 formed and deposited in the positive half-cell will block the tubes, bring increasing pressure internally and cause electrolyte leakage. That is the reason why VFB-80/50 and VFB-160/50 stop running unplanned and the infeasibility in detecting the average valence at the end.

The profile of the discharge capacity retention (showed in Fig. 3 (a, e)) after the mix process can be separated into a rising segment and a descending segment. In the rising segment, the discharge capacity retentions keep increasing and then reach the summit. Furthermore, every time after the mix process in a VFB, it takes more cycles than before for the discharge capacity retention to reach the summit. Then, in the descending segment, the discharge capacity retentions keep decreasing. Associating with the average valences and volume changes showed in Fig. 3(b–d, f–h), a schematic diagram is made and showed in Fig. 4 to illustrate the composition changes of the electrolytes during cycle number test.

As displayed in Fig. 4(a), the initial electrolyte containing 1.5 M vanadium ion (V^{3+}/VO^{2+} = 1:1) turns to tetravalence at the positive side and trivalence at the negative side after pre-charge process (showed in Fig. 4(b)). In the ideal case (ignoring side reactions and permeation of vanadium ions), after the charge process showed in Fig. 4(c), when VO^{2+} ions are oxidized into VO_2^+ ions in the positive electrolyte, an equal number of V^{3+} ions are reduced to V^{2+} ions in the negative electrolyte. Then the reverse reactions occur in the discharge process, the valences of ions turn back to the state before charge process (as displayed in Fig. 4(d)). However, in fact, the non-equilibrium transfer rates of vanadium ions lead to concentration of vanadium decrease in the negative electrolyte and increase in the positive electrolyte [24]. Therefore, as displayed in Fig. 4(e), the net transferred vanadium ions with lower valence accumulates in the positive electrolyte. In that case, the discharge capacity can be fully recovered by mixing the positive and negative electrolytes. Nevertheless, elevated average valence caused by side reactions weakens the function of the mix process.

As illustrated in Fig. 4(f), the average valence of mixed electrolyte is higher than that of the initial electrolyte, which means the equally divided electrolytes in the positive and negative reservoirs contain excess VO^{2+} ions. In that case, after the pre-charge process (showed in Fig. 4(g)), when almost all the V^{3+} ions are oxidized to VO^{2+} ions in the positive electrolyte, there are still remaining VO^{2+} ions that are not reduced to V^{3+} ions in the negative electrolyte. Then, after the charge process (showed in Fig. 4(h)), near all the VO^{2+} ions are oxidized into VO_2^+ at the positive side

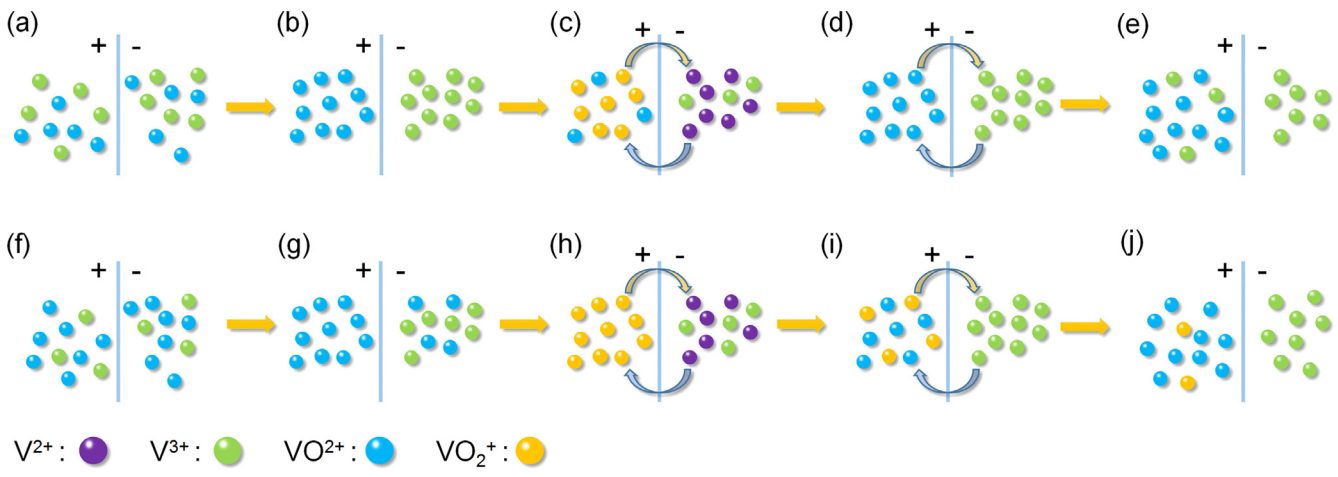

Fig. 4. (a, f) Schematic diagrams of the composition in the initial and the mixed electrolytes; (b, g) The composition of the positive and negative electrolytes after pre-charge process; (c, d, h, i) The changes of the active vanadium ions during charge-discharge cycling process; (e, j) The concentration-imbalanced electrolytes caused by the permeation of vanadium ions.

while relatively low concentration of V^{2+} ions are formed at the negative side, as part of the electrons are consumed in the reduction of the excess VO^{2+} ions at the negative side. Consequently, in the selected voltage window, part of the VO_2^+ ions in the positive electrolyte cannot join the electrochemical reactions during discharge process, for the shortage of V^{2+} ions (displayed in Fig. 4(i)). Although there are free V^{3+} ions, the discharge capacity is limited by the concentration of available V^{2+} ions in the negative electrolyte. Owing to higher permeability of V^{3+} and V^{2+} ions, net vanadium ions transfer from the negative to the positive side through Nafion 115 membrane, which has two contrary consequences: (a) In the positive electrolyte, the remaining VO_2^+ ions react with transferred V^{3+} and V^{2+} ions (illustrated in Fig. 4(j)); in the negative electrolyte, the V^{3+} ions that are absent from the electrochemical reactions before will be reduced into V^{2+} ions and rejoin into charge-discharge cycling process. Consequence (a) leads to the rise of the discharge capacity. (b) The non-equilibrium permeability of vanadium ions causes the decrease of total vanadium concentration in the negative electrolyte, leading to the decay of the discharge capacity [49]. After the mix process, consequence (a) plays a major role at first, thus the discharge capacity increases. With the change of the electrolyte composition, there will be a balance between consequence (a) and (b), so the discharge capacity reaches the summit. Then the consequence (b) dominates, and the discharge capacity decreases. This explains the rising and descending segment in Fig. 3(a, e). Besides, when the average valance of electrolyte gets higher than before, it takes more time for the components of the mixed electrolyte to reach a new balance, so prolonged rising segments are observed.

From the results in Figs. 3 and 4, it can be summarized that the mix process can regenerate the discharge capacity significantly, but the elevated average valence weakens the benefit of the mix method. Inspired by the rebalance cell used for capacity restoration of iron-chromium redox flow batteries [57], we are working on adjusting the average valence of mixed electrolyte by online electrolysis with an extra electrolysis cell. Thus, the valence issue caused by side reactions and gas leakages may be minimized by online electrolysis. This will be introduced in our future work.

3.2. Cell performance

The coulomb efficiencies (CE), voltage efficiencies (VE) and energy efficiencies (EE) of VFB-80, VFB-80/75, VFB-80/50, VFB-160, VFB-160/75 and VFB-160/50 are displayed in Fig. 5. Fig. 5(a–c) shows the efficiencies of VFB-80, VFB-80/75 and VFB-80/50 and Fig. 5(d–f) shows the efficiencies of VFB-160, VFB-160/75 and VFB-160/50. During the whole experiment process, the CE values are near 93% under current the density of 80 mA cm^{-2} and near

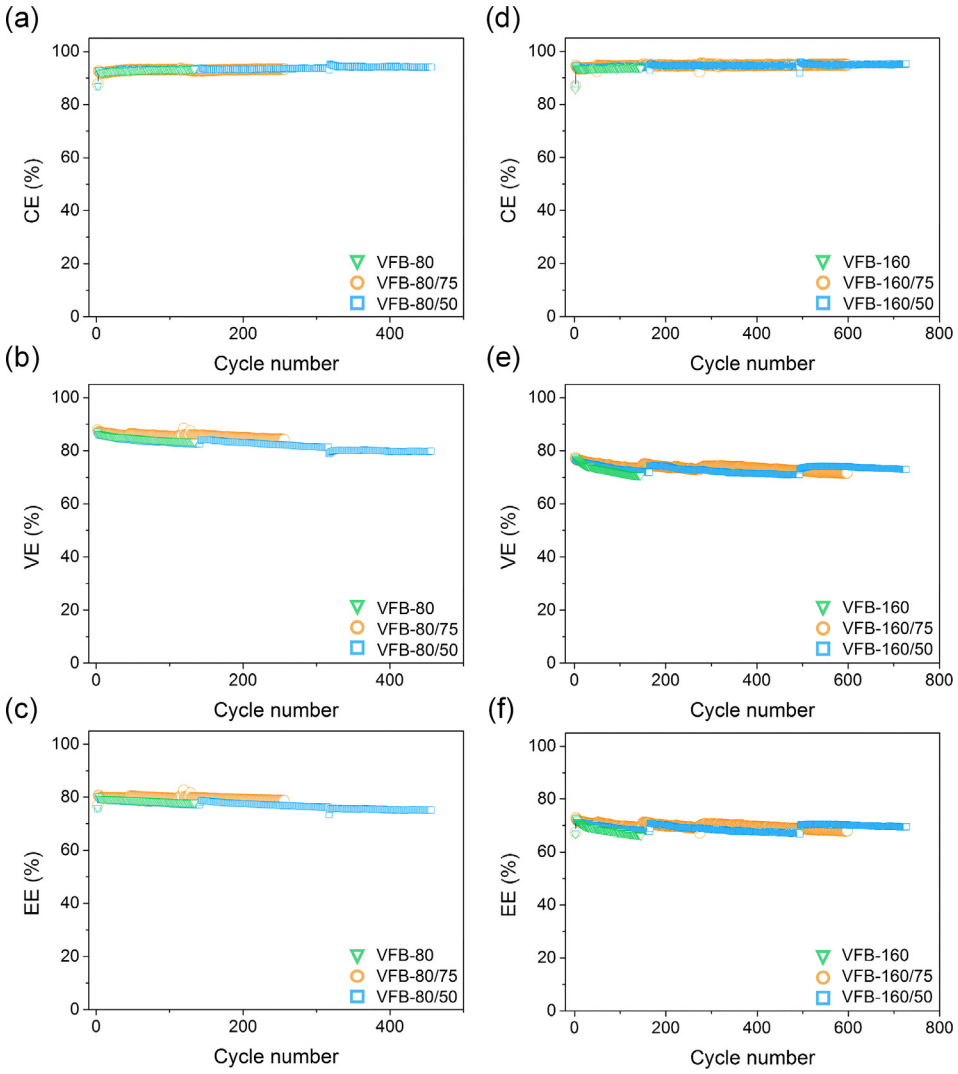

Fig. 5. Efficiencies of all six VFBs during the charge-discharge cycling process at 80 mA cm^{-2} (a–c) and 160 mA cm^{-2} (d–f).

94% under the current density of 160 mA cm^{-2}. A mild improvement (about 0.7%) of CE is recorded at cycle 317 in VFB-80/50, similarly, this slightly improvements occur in VFB-160/75 and VFB-160/50 every time after the mix process. As CE is mainly determined by the crossover of vanadium ions through Nafion 115 membrane, it may be ascribed to the suppression of the non-equilibrium transfer of vanadium ions caused by the changed composition of the mixed electrolyte [29].

As to VE, improvements are recorded at cycle 42 and 113 in VFB-80/75; at cycle 50, 149 and 274 in VFB-160/75; at cycle 165 and 494 in VFB-160/50. But the improvement only occurs at cycle 142 while a decline happens at cycle 317 in VFB-80/50. As the possibly formed precipitation of V_2O_5 can deposit on the surface of Nafion 115 membrane and the gap in the graphite felts, an undesirable increase of resistance leads to VE decay. The decay is partially recovered during the mix process as the V^{3+} ions existed in the negative electrolyte flow into the positive half-cell and react with the precipitation of V_2O_5. But with higher average valence of vanadium ions in the mixed electrolyte, the V^{3+} ions are not enough for consuming the precipitation of V_2O_5. Moreover, the excess VO_2^+ ions formed during the pre-charge and charge processes endow the precipitation problem. Thus, increases of VE values after mix processes are only recorded at cycle 142 in VFB-80/50. Besides the precipitation of V_2O_5, the degeneration of the oxygen-containing functional groups on the surface of graphite electrode can also cause the decrease of VE during the cycle number test. Moreover, this degeneration is unrecoverable during the test.

The variation tendency of EE has almost as much in common with VE, as EE can be obtained by calculating the product of CE and VE.

3.3. Charge-discharge curves

Fig. 6 shows the charge-discharge curves of VFB-160/75 before and after mixing the positive and negative electrolytes. Both the resistance of the cell and the practical electrode potential can affect the charge and discharge voltages. The discharge voltage increases after the first and the second mix processes may be mainly caused by the decreased resistance, as consuming the precipitation of V_2O_5 on the membrane and electrode during mix process can reduce the resistance of the cell (corroborated by the VE changes in Fig. 5). Therefore, the almost unchanged discharge voltage after the third mix process can be ascribed to the weakened contribution of mix process in consuming the precipitation of V_2O_5 when the average valence increases to near tetravalence. Comparing the charge voltages in Fig. 6(a–c), each time after mix process, the charge voltages increase. Despite the reduced resistance of cell can lead to charge voltages decrease, the increases may mainly owe to the changed practical electrode potential. The discharge capacities increase more or less after the first and the second mix processes, but decrease after the third mix process.

Associating with the changes of the average valence, the discharge capacity retention and the cell performance in Figs. 3 and 4, it can be concluded that the mix process can regenerate discharge capacity and recover VFB performance when the average valence is relatively low, and become useless or even harmful to discharge capacity and VFB performance when the average valence increases to near tetravalence.

3.4. Cycle number, total discharge capacity and average discharge capacity

In order to evaluate the function of this mix method, the cycle numbers, the total discharge capacities and the average discharge capacities of all six VFBs are calculated and showed in Fig. 7. The total discharge capacity is the sum of all the discharge capacities of a VFB during cycle number test and the average discharge capacity is the total discharge capacity divided by the cycle number. The associated calculation of VFB-80/50 ends at cycle 316 because the discharge capacity retentions of VFB-80/50 after the second mix process are lower than 50%.

With this mix method, the cycle number is increased from 134 (VFB-80) to 256 (VFB-80/75) and 316 (VFB-80/50) at the current density of 80 mA cm^{-2}, and is increased from 145 (VFB-160) to

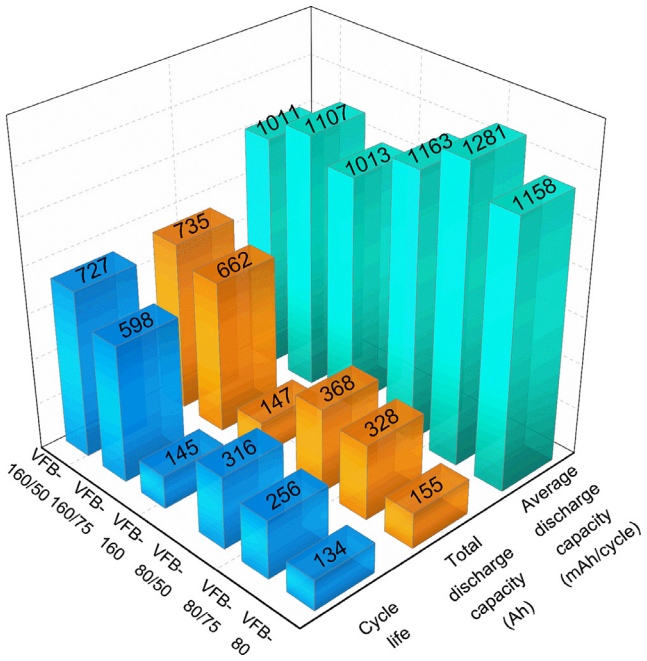

Fig. 7. Cycle lives, total discharge capacity/Ah and average discharge capacity/mAh $cycle^{-1}$ of VFBs.

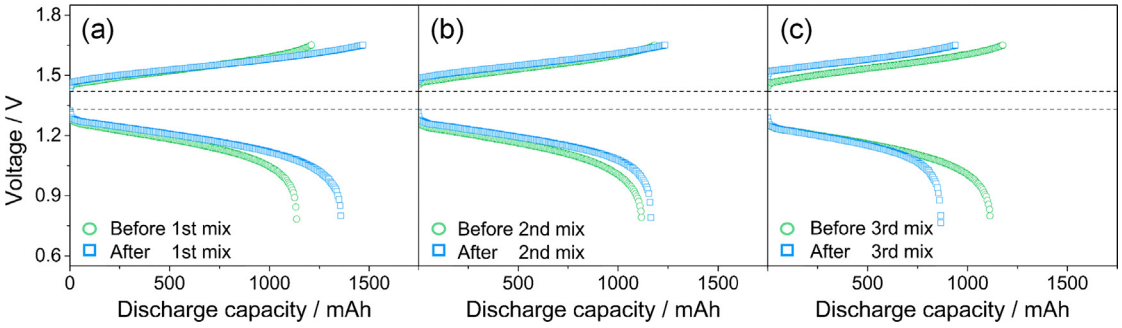

Fig. 6. Charge-discharge curves of VFB-160/75 before and after the first mix process (a), the second mix process (b) and the third mix process (c).

598 (VFB-160/75) and 727 (VFB-160/50) at the current density of 160 mA cm^{-2}. The total discharge capacity is increased from 155 Ah (VFB-80) to 328 Ah (VFB-80/75) and 368 Ah (VFB-80/50) at the current density of 80 mA cm^{-2}, and is increased from 147 Ah (VFB-160) to 662 Ah (VFB-160/75) and 735 Ah (VFB-160/50) at the current density of 160 mA cm^{-2}. Besides the benefits in prolonging the cycle number, the mix method can provide equivalent (at the discharge capacity retention of 50%) or better (at the discharge capacity retention of 75%) average discharge capacity.

In summary, not only the mix method has significant benefit in prolonging battery cycle number, but also it offers equivalent or better average discharge capacity of each cycle. The proper time of mix can be determined by the consideration of maintenance frequency and discharge capacity requirement.

4. Conclusions

In this study, different current densities (80 and 160 mA cm^{-2}) and mix time (at the discharge capacity retention of 75% and 50%) are chosen to investigate the benefits and limitations of the mix method, also the mechanism of the discharge capacity behavior is discussed. By mixing the positive and negative electrolytes at the discharge capacity retention of 75%, the cycle number is increased from 134 to 256 at the current density of 80 mA cm^{-2}, and is increased from 145 to 598 at the current density of 160 mA cm^{-2}. Meanwhile, the average discharge capacity is increased from 1158 mAh $cycle^{-1}$ to 1281 mAh $cycle^{-1}$ at the current density of 80 mA cm^{-2}, and is increased from 1013 mAh $cycle^{-1}$ to 1107 mAh $cycle^{-1}$ at the current density of 160 mA cm^{-2}. The result shows that the mix method has great benefits in prolonging cycle number and improving total discharge capacity without decreasing the average discharge capacity. Although the elevated valence of mixed electrolyte caused by side reactions and possible gas leakage limits the benefits of the mix method. This drawback can be alleviated by employing online electrolysis. In conclusion, the mix method is an uncomplicated, economic and effective technique for regenerating the capacities of VFBs, and has potential contribution to sustainable development and resource conservation.

Acknowledgements

This research was made possible with the financial support from Shenzhen Basic Research Project (JCYJ20150331151358142, JCYJ20170307153749357), Natural Science Foundation of Guangdong Province (2015A030313794) and National Natural Science Foundation of China (61308119).

References

[1] Dong X, Chen L, Liu J, Haller S, Wang Y, Xia Y. Environmentally-friendly aqueous Li (or Na)-ion battery with fast electrode kinetics and super-long life. Sci Adv 2016;2:e1501038.
[2] Jia C, Pan F, Zhu YG, Huang Q, Lu L, Wang Q. High–energy density nonaqueous all redox flow lithium battery enabled with a polymeric membrane. Sci Adv 2015;1:e1500886.
[3] Sun Y, Liu N, Cui Y. Promises and challenges of nanomaterials for lithium-based rechargeable batteries. Nat Energy 2016;1:16071.
[4] Lukatskaya MR, Dunn B, Gogotsi Y. Multidimensional materials and device architectures for future hybrid energy storage. Nat Commun 2016;7:12647.
[5] Seh ZW, Sun Y, Zhang Q, Cui Y. Designing high-energy lithium-sulfur batteries. Chem Soc Rev 2016;45:5605–34.
[6] Li L, Kim S, Wang W, Vijayakumar M, Nie Z, Chen B, et al. A stable vanadium redox-flow battery with high energy density for large-scale energy storage. Adv Energy Mater 2011;1:394–400.
[7] Winsberg J, Hagemann T, Janoschka T, Hager MD, Schubert US. Redox-flow batteries: from metals to organic redox-active materials. Angew Chem Int Ed 2017;56:686–711.
[8] Noack J, Roznyatovskaya N, Herr T, Fischer P. The chemistry of redox-flow batteries. Angew Chem Int Ed 2015;54:9776–809.
[9] Dunn B, Kamath H, Tarascon J-M. Electrical energy storage for the grid: a battery of choices. Science 2011;334:928–34.
[10] Wang W, Luo Q, Li B, Wei X, Li L, Yang Z. Recent progress in redox flow battery research and development. Adv Funct Mater 2013;23:970–86.
[11] Skyllas-Kazacos M, Chakrabarti MH, Hajimolana SA, Mjalli FS, Saleemd M. Progress in flow battery research and development. J Electrochem Soc 2011;158(8):R55–R79.
[12] Skyllas-Kazacos M. New all-vanadium redox flow cell. J Electrochem Soc 1986;133:1057.
[13] Skyllas-Kazacos M, Cao L, Kazacos M, Kausar N, Mousa A. Vanadium electrolyte studies for the vanadium redox battery-a review. ChemSusChem 2016;9:1521–43.
[14] Zeng YK, Zhao TS, An L, Zhou XL, Wei L. A comparative study of all-vanadium and iron-chromium redox flow batteries for large-scale energy storage. J Power Sources 2015;300:438–43.
[15] Choi C, Kim S, Kim R, Choi Y, Kim S, H-y Jung, et al. A review of vanadium electrolytes for vanadium redox flow batteries. Renew Sust Energ Rev 2017;69:263–74.
[16] Xi J, Xiao S, Yu L, Wu L, Liu L, Qiu X. Broad temperature adaptability of vanadium redox flow battery – Part 2: cell research. Electrochim Acta 2016;191:695–704.
[17] Jiang B, Yu L, Wu L, Mu D, Liu L, Xi J, et al. Insights into the impact of the nafion membrane pretreatment process on vanadium flow battery performance. ACS Appl Mater Interfaces 2016;8:12228–38.
[18] Zhou XL, Zeng YK, Zhu XB, Wei L, Zhao TS. A high-performance dual-scale porous electrode for vanadium redox flow batteries. J Power Sources 2016;325:329–36.
[19] Xi J, Zhang W, Li Z, Zhou H, Liu L, Wu Z, et al. Effect of electro-oxidation current density on performance of graphite felt electrode for vanadium redox flow battery. Int J Electrochem Sci 2013;8:4700–11.
[20] Leung P, Li X, Ponce de León C, Berlouis L, Low CTJ, Walsh FC. Progress in redox flow batteries, remaining challenges and their applications in energy storage. RSC Adv 2012;2:10125.
[21] Alotto P, Guarnieri M, Moro F. Redox flow batteries for the storage of renewable energy: a review. Renew Sustain Energy Rev 2014;29:325–35.
[22] Kear G, Shah AA, Walsh FC. Development of the all-vanadium redox flow battery for energy storage: a review of technological, financial and policy aspects. Int J Energy Res 2012;36:1105–20.
[23] Xiao S, Yu L, Wu L, Liu L, Qiu X, Xi J. Broad temperature adaptability of vanadium redox flow battery—Part 1: electrolyte research. Electrochim Acta 2016;187:525–34.
[24] Luo Q, Li L, Wang W, Nie Z, Wei X, Li B, et al. Capacity decay and remediation of nafion-based all-vanadium redox flow batteries. ChemSusChem 2013;6:268–74.
[25] Derr I, Fetyan A, Schutjajew K, Roth C. Electrochemical analysis of the performance loss in all vanadium redox flow batteries using different cut-off voltages. Electrochim Acta 2017;224:9–16.
[26] Zhou XL, Zhao TS, An L, Zeng YK, Wei L. Critical transport issues for improving the performance of aqueous redox flow batteries. J Power Sources 2017;339:1–12.
[27] Sukkar T, Skyllas-Kazacos M. Water transfer behaviour across cation exchange membranes in the vanadium redox battery. J Membr Sci 2003;222:235–47.
[28] Cao L, Kronander A, Tang A, Wang D-W, Skyllas-Kazacos M. Membrane permeability rates of vanadium ions and their effects on temperature variation in vanadium redox batteries. Energies 2016;9:1058.
[29] Zhou XL, Zhao TS, An L, Zeng YK, Yan XH. A vanadium redox flow battery model incorporating the effect of ion concentrations on ion mobility. Appl Energy 2015;158:157–66.
[30] Boettcher PA, Agar E, Dennison CR, E. Caglan Kumburd Z. Modeling of ion crossover in vanadium redox flow batteries: a computationally-efficient lumped parameter approach for extended cycling. J Electrochem Soc 2016;163:(1) A5244-A52.
[31] Tang A, Bao J, Skyllas-Kazacos M. Thermal modelling of battery configuration and self-discharge reactions in vanadium redox flow battery. J Power Sources 2012;216:489–501.
[32] Tang A, Bao J, Skyllas-Kazacos M. Dynamic modelling of the effects of ion diffusion and side reactions on the capacity loss for vanadium redox flow battery. J Power Sources 2011;196:10737–47.
[33] Yang X-G, Ye Q, Cheng P, Zhao TS. Effects of the electric field on ion crossover in vanadium redox flow batteries. Appl Energy 2015;145:306–19.
[34] Ngamsai K, Arpornwichanop A. Measuring the state of charge of the electrolyte solution in a vanadium redox flow battery using a four-pole cell device. J Power Sources 2015;298:150–7.
[35] Wei Z, Tseng KJ, Wai N, Lim TM, Skyllas-Kazacos M. Adaptive estimation of state of charge and capacity with online identified battery model for vanadium redox flow battery. J Power Sources 2016;332:389–98.
[36] Liu L, Xi J, Wu Z, Zhang W, Zhou H, Li W, et al. State of charge monitoring for vanadium redox flow batteries by the transmission spectra of V(IV)/V(V) electrolytes. J Appl Electrochem 2012;42:1025–31.
[37] Luo Q, Li L, Nie Z, Wang W, Wei X, Li B, et al. In-situ investigation of vanadium ion transport in redox flow battery. J Power Sources 2012;218:15–20.
[38] Roznyatovskaya N, Herr T, Küttinger M, Fühl M, Noack J, Pinkwart K, et al. Detection of capacity imbalance in vanadium electrolyte and its electrochemical regeneration for all-vanadium redox-flow batteries. J Power Sources 2016;302:79–83.

[39] Liu L, Li Z, Xi J, Zhou H, Wu Z, Qiu X. Rapid detection of the positive side reactions in vanadium flow batteries. Appl Energy 2017;185:452–62.
[40] Wei L, Zhao TS, Xu Q, Zhou XL, Zhang ZH. In-situ investigation of hydrogen evolution behavior in vanadium redox flow batteries. Appl Energy 2017;190:1112–8.
[41] Yuan Z, Zhu X, Li M, Lu W, Li X, Zhang H. A highly ion-selective zeolite flake layer on porous membranes for flow battery applications. Angew Chem Int Ed 2016;55:3058–62.
[42] Zhao Y, Yuan Z, Lu W, Li X, Zhang H. The porous membrane with tunable performance for vanadium flow battery: the effect of charge. J Power Sources 2017;342:327–34.
[43] Yuan Z, Duan Y, Zhang H, Li X, Zhang H, Vankelecom I. Advanced porous membranes with ultra-high selectivity and stability for vanadium flow batteries. Energy Environ Sci 2016;9:441–7.
[44] Li X, Zhang H, Mai Z, Zhang H, Vankelecom I. Ion exchange membranes for vanadium redox flow battery (VRB) applications. Energy Environ Sci 2011;4:1147.
[45] Xi J, Li Z, Yu L, Yin B, Wang L, Liu L, et al. Effect of degree of sulfonation and casting solvent on sulfonated poly(ether ether ketone) membrane for vanadium redox flow battery. J Power Sources 2015;285:195–204.
[46] Mu D, Yu L, Liu L, Xi J. Rice paper reinforced sulfonated poly(ether ether ketone) as low-cost membrane for vanadium flow batteries. ACS Sustain Chem Eng 2017;5:2437–44.
[47] Zhou XL, Zhao TS, An L, Zeng YK, Zhu XB. Performance of a vanadium redox flow battery with a VANADion membrane. Appl Energy 2016;180:353–9.
[48] Li B, Luo Q, Wei X, Nie Z, Thomsen E, Chen B, et al. Capacity decay mechanism of microporous separator-based all-vanadium redox flow batteries and its recovery. ChemSusChem 2014;7:577–84.
[49] Park JH, Park JJ, Park OO, Yang JH. Capacity decay mitigation by asymmetric positive/negative electrolyte volumes in vanadium redox flow batteries. ChemSusChem 2016;9:3181–7.
[50] Yan L, Li D, Li S, Xu Z, Dong J, Jing W, et al. Balancing osmotic pressure of electrolytes for nanoporous membrane vanadium redox flow battery with a draw solute. ACS Appl Mater Interfaces 2016;8:35289–97.
[51] Agar E, Benjamin A, Dennison CR, Chen D, Hickner MA, Kumbur EC. Reducing capacity fade in vanadium redox flow batteries by altering charging and discharging currents. J Power Sources 2014;246:767–74.
[52] Wang K, Liu L, Xi J, Wu Z, Qiu X. Reduction of capacity decay in vanadium flow batteries by an electrolyte-reflow method. J Power Sources 2017;338:17–25.
[53] Mohamed MR, Leung PK, Sulaiman MH. Performance characterization of a vanadium redox flow battery at different operating parameters under a standardized test-bed system. Appl Energy 2015;137:402–12.
[54] Dai W, Shen Y, Li Z, Yu L, Xi J, Qiu X. SPEEK/graphene oxide nanocomposite membranes with superior cyclability for highly efficient vanadium redox flow battery. J Mater Chem A 2014;2:12423.
[55] Li Z, Dai W, Yu L, Liu L, Xi J, Qiu X, et al. Properties investigation of sulfonated poly(ether ether ketone)/polyacrylonitrile acid-base blend membrane for vanadium redox flow battery application. ACS Appl Mater Interfaces 2014;6:18885–93.
[56] Zhang W, Liu L, Liu L. An on-line spectroscopic monitoring system for the electrolytes in vanadium redox flow batteries. RSC Adv 2015;5:100235–43.
[57] Zeng YK, Zhao TS, Zhou XL, Zou J, Ren YX. A hydrogen-ferric ion rebalance cell operating at low hydrogen concentrations for capacity restoration of iron-chromium redox flow batteries. J Power Sources 2017;352:77–82.